Power Allocation for Uplink Communications of Massive Cellular-Connected UAVs

Xuesong Cai, *Member, IEEE,* István Z. Kovács, *Member, IEEE,* Jeroen Wigard, Rafhael Amorim,
Fredrik Tufvesson, *Fellow, IEEE,* and Preben E. Mogensen

Abstract—Cellular-connected unmanned aerial vehicle (UAV) has attracted a surge of research interest in both academia and industry. To support aerial user equipment (UEs) in the existing cellular networks, one promising approach is to assign a portion of the system bandwidth exclusively to the UAV-UEs. This is especially favorable for use cases where a large number of UAV-UEs are exploited, e.g., for package delivery close to a warehouse. Although the nearly line-of-sight (LoS) channels can result in higher powers received, UAVs can in turn cause severe interference to each other in the same frequency band. In this contribution, we focus on the uplink communications of massive cellular-connected UAVs. Different power allocation algorithms are proposed to either maximize the minimal spectrum efficiency (SE) or maximize the overall SE to cope with the severe interference based on the successive convex approximation (SCA) principle. One of the challenges is that a UAV can affect a large area meaning that many more UAV-UEs must be considered in the optimization problem, which is essentially different from that for terrestrial UEs. The necessity of single-carrier uplink transmission further complicates the problem. Nevertheless, we find that the special property of large coherent bandwidths and coherent times of the propagation channels can be leveraged. The performances of the proposed algorithms are evaluated via extensive simulations in the full-buffer transmission mode and bursty-traffic mode. Results show that the proposed algorithms can effectively enhance the uplink SEs. This work can be considered the first attempt to deal with the interference among massive cellular-connected UAV-UEs with optimized power allocations.

Index terms— Interference, power control, geometrical programming, successive convex approximation, and UAV communications.

I. INTRODUCTION

Due to the rapid development of unmanned aerial vehicles (UAVs) in reducing their costs, sizes, weights and energy consumption, the UAV assistance paradigm [1], i.e., using UAVs to support many applications and terrestrial networks, users, and communicating entities, has attracted significant attention. Specifically, deployed as aerial base stations (BSs) [2], UAVs can quickly provide wireless connections, e.g., in the damaged areas after disasters for rescue purposes. By leveraging the nearly line-of-sight (LoS) radio propagation channels, UAVs can also be utilized as relays to enable energy-efficient sensing, internet-of-things and coverage improvement [3]–[5]. Moreover, other applications such as network optimization, smart agriculture, forest monitoring, goods delivery, etc. [6], [7] are becoming autonomous and convenient with the help of UAVs. Meanwhile, UAVs as new aerial user equipments (UEs) connected to the existing cellular networks, i.e., cellular-connected UAVs [8], [9], have been identified as an important paradigm shift. The current almost everywhere cellular networks are expected to provide reliable command and control (C2) and high-throughput payload communications for UAV-UEs to enable, e.g., beyond visual LoS flight tasks and high-definition video streaming. However, although the nearly LoS channels are advantageous to receive higher powers, UAVs can in turn cause severe interference. This becomes more critical with the rapid growth of the number of UAVs that are connected to cellular networks, significantly affecting the connectivity of both aerial and terrestrial UEs.

Different techniques have been investigated to provide reasonable services to UAVs and terrestrial UEs. In [8], [10], [11], the authors proposed to exploit massive multiple-input-multiple-output (MIMO) available at BS side to point beams towards intended UEs and more sophistically place spatial nulls to UEs in other cells that are vulnerable to the interference. In such a way, beamforming gain and spatial multiplexing gains can be harvested to improve wireless connectivity. Although massive MIMO at BS is promising, it requires large investments and takes time to upgrade the infrastructure. As a cheaper and fast alternative, implementing a beamforming system or directional antennas on board the UAV was proposed in [12], [13]. The authors have shown its effectiveness to increase the uplink performance of UAV communications. In [14], the authors proposed to exploit the passive beamforming of intelligent reflecting surfaces (IRSs) to achieve an optimal performance tradeoff between UAV-UEs and terrestrial UEs. In [15], a deep Q-learning framework is utilized to tune the standard fixed power allocation algorithm for the UAV to mitigate interference, which requires the UAV to only update its coordinates and received signal-to-interference-plus-noise ratio (SINR) continuously. In [16], the effectiveness of three different interference mitigation methods including power control, beamforming and coordinated multi-point transmission was compared. In [17], the authors considered the case of one BS serving a cluster of UAVs, and the sum rate or the minimum rate of UAVs was optimized by power control. The authors in [18] investigated the uplink SINR distribution

of UAV-UEs and terrestrial UEs based on the technique of stochastic geometry. It is found that there exists an optimal height of UAVs for SINR enhancement. In [19], by jointly optimizing the UAV's uplink cell associations and power allocations, the weighted sum rate of the UAV and terrestrial UEs was optimized. In [20], idle BSs without serving any other UEs in the UAV's communication channel were exploited to help co-channel BSs mitigate the interference. In [21], a cooperative interference cancellation strategy that exploits the existing backhaul links among BSs was proposed for sum-rate maximization. Specifically, a multi-antenna UAV sends multiple data streams to its serving BSs, which are then forwarded to the backhaul-connected BSs that serve terrestrial UEs for interference cancellation. In [22], the authors provided a good summary of different interference coordination and mitigation algorithms for the coexistence of UAV-UEs and terrestrial UEs. A comparison of the above works is shown in Table I.

Although the above-mentioned approaches have demonstrated potential in improving the performance of serving flying UAVs and protecting terrestrial UEs, *they do not well consider the case where the density of UAVs is very high,* which is probable in the near future. The basic assumption in these investigations, e.g. [13], [19], [20], [22], is that only a few (even only one) UAVs exist in a large area. However, as predicted by Federal Aviation Administration (FAA), the number of commercial UAV fleets can reach up to 1.6 million by 2024 [23], [24]. In [25], a typical use case of cellular-connected UAVs is recognized as the package delivery, e.g., the Amazon Prime Air project in the early stage, with a medium to high UAV density. It is estimated that several UAVs can exist per square mile near to the warehouse or operations center around 2022, which means that each cell (in the hotspot areas) can have several active UAV-UEs. Developing robust interference mitigation techniques for *massive* UAV-UEs deployment scenarios is also considered a key open problem in [26]. *Therefore, identified as an important communication scenario that has seldomly been addressed in the literature, we in this work focus on the uplink communication for UAV-UEs of high densities, i.e., a massive number of UAV-UEs.*

Due to the nearly-LoS channels, these UAV-UEs can cause severe interference to terrestrial UEs in a rather large area. As demonstrated in [26], the connectivity probability of terrestrial UEs can be lowered significantly, e.g. from 0.95 to 0.7 with the number of UAVs increasing. To avoid the many UAVs negatively affecting the performance of terrestrial UEs, we assume, similarly as discussed in [11], [27], that UAV-UEs and terrestrial UEs use orthogonal resource blocks (RBs) in each transmission interval as illustrated in Fig. 1. This spectrum sharing has been suggested in [28] as the most suitable strategy for maintaining a guaranteed rate for UAVs and high performance of terrestrial UEs if the number of UAVs is large. The investigation in [11] also shows its effectiveness. In [29], the authors also suggest the necessity in the future of dedicated air-to-ground (A2G) cellular networks without serving terrestrial UEs. Therefore, the crux we aim to solve in this work is to optimize the uplink performance of a large number of
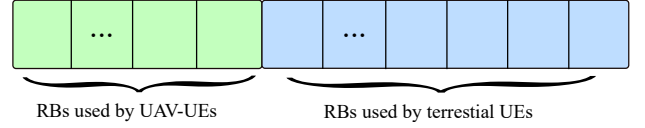

Fig. 1: UAV-UEs and terrestrial UEs use orthogonal RBs.

UAVs, coping with the inter-cell interference among them. It is worth noting that although the problem seems similar to the conventional case where all UEs are terrestrial and different algorithms [30]–[35] are available in the literature with local optimal solutions, *it does differ mainly in two aspects. i) The A2G channels between the UAV-UEs and BSs are nearly LoS. This bring new properties and performance behavior of UAVs; ii) Many more, e.g., tens or even up to hundreds of cells need to be considered compared to only a few cells in the terrestrial case, which can lead to exponentially increasing complexity.* To this end, the main contributions and novelties of this paper are summarized as follows:

- To deal with the exponential complexity caused by the massive number of UAVs in the optimization problem, a novel successive convex approximation (SCA) technique is applied based on the principle of geometrical programming (GP).
- By exploiting the special characteristics of the nearly LoS UAV propagation channels, different algorithms applied in the frequency domain and/or the time domain are proposed to optimize the spectrum efficiency (SE) of the system. The important and practical constraint, i.e., uplink single-carrier (SC) constraint[1], is also considered.
- Extensive simulations are performed to evaluate the performances of the proposed algorithms. Both full-buffer transmission and bursty-traffic modes are considered. Moreover, clustered application of the algorithms is also discussed in compromising between performance and signaling overhead. The numerical results show the effectiveness of these algorithms and provide important insights into the practical system design.

The rest of this paper is structured as follows. In Sect. II, low altitude A2G channel properties and preliminary understanding of the uplink UAV communications are discussed. In Sect. III, different power allocation algorithms are proposed and elaborated. Sect. IV presents the extensive simulations in full-buffer transmission mode and bursty-traffic mode for evaluating the proposed algorithms. Detailed discussions are also included. Finally, conclusive remarks are given in Sect. V.

---

[1]Orthogonal Frequency Division Multiple Access (OFDMA) has been a standard radio access technique in 4G LTE and 5G networks. However, a major issue of OFDMA is a high peak-to-average power ratio (PAPR), which is unfriendly to mobile UEs whose power consumption is a key consideration. Thus, SC-OFDMA with significantly lower PAPR has been an alternative for mobile UEs for uplink transmission. Because the waveform is essentially single-carrier, the occupied bandwidth has to be continuous and with the same power level, which is the SC constraint considered herein.

Table I: Investigations of interference mitigation for cellular-connected UAVs.

References	Techniques	Methodology	UE types
[8], [10], [11]	Massive MIMO, beamforming, spatial nulling	Simulations	UAV-UEs and terrestrial UEs
[12], [13]	Directional antennas onboard a UAV	Measurement verification	One UAV and terrestrial UEs
[14]	IRSs, passive beamforming	Sum-rate optimization	One UAV and terrestrial UEs
[15]	Power control	Deep Q-learning	UAVs
[16], [22]	Power control, beamforming, coordinated multipoint, frequency reuse, interference cancellation, etc.	Simulations	Several UAV-UEs and terrestrial UEs
[19]	Uplink cell association, power control	Weighted sum-rate optimization	One UAV and terrestrial UEs
[20], [21]	Backhaul, multi-beam UAV, cooperative interference cancellation	Weighted sum-rate optimization	One UAV and terrestrial UEs

II. THE UPLINK COMMUNICATIONS OF MASSIVE CELLULAR-CONNECTED UAVs

In this section, we discuss the characteristics of the propagation channels among UAVs and terrestrial BSs, and a preliminary analysis of power allocation, interference and scheduling is also included.

A. Low altitude A2G propagation channels

Many measurement-based investigations such as [36]–[40] have demonstrated that the A2G propagation channels at higher heights are nearly LoS. For example, 3GPP [36] suggests a LoS probability of 1 for rural areas and moderately high UAV altitude larger than 40 m, which is also verified by the measurements in [40] for even lower heights. In [37], path loss exponents (PLEs) were found to be almost free-space values as 2.1 and 2 at 60 m and 120 m, respectively. In [38], [39], the Rician K-factors of the A2G channels were found to be large for most cases at higher heights with a mean value around 15 dB. Although in few cases, the K-factor could be smaller due to, e.g., the reflections from buildings [39], [40] in urban or industrial areas, spatial analysis in [40] for the A2G channels has shown that the additional cluster(s) are usually separable to the LoS cluster in the azimuth domain with angle differences larger than 60°. This means that if a UAV is equipped with directional antennas, even the channel with several clusters can probably be simplified as a single-cluster channel with a high K-factor. This is a reasonable expectation since as shown in Fig. 4 in Sect. II-B, using omnidirectional antennas onboard UAVs can cause rather severe interference. The authors in [13] exploited an array consisting of six directional antennas each with a half-power-beamwidth (HPBW) of 60° to cover the whole 360° azimuth, and the best antenna was triggered for the communication. This relatively simple and low-cost switching strategy of directional antennas was able to significantly improve the performance. Given the above reasoning, it can be inferred that the nearly LoS or single-cluster A2G channels are quite flat in a certain bandwidth. This has also been demonstrated by the ultra-wideband A2G channel measurements [41] where the coherent bandwidths of the channels are found to be at least 100 MHz at different scenarios and heights. Moreover, for the same reasons and the relatively low speeds of low-altitude UAVs, the A2G channels have relatively large coherent time, e.g. tens of ms or even longer [42]. For example, for 20 LTE symbols that last less than 2 ms, a UAV at a speed of 10 m/s moves less than 2 cm,
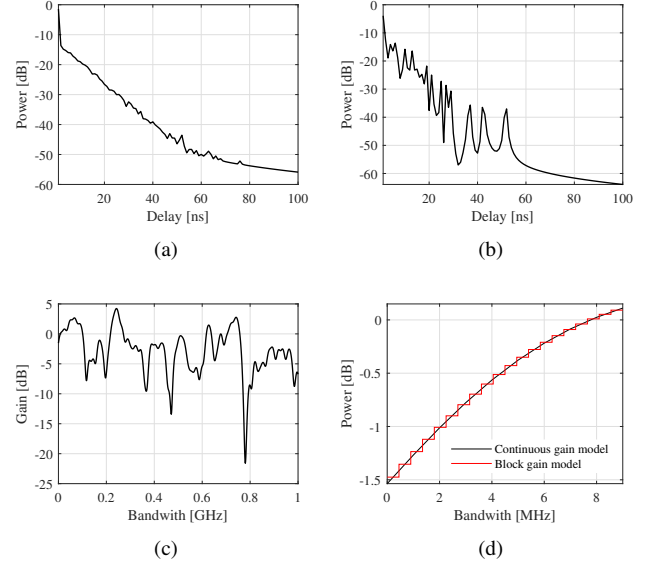

Fig. 2: Tapped-delay-line channel model. (a) Power delay profile. (b) A realization of the channel. (c) Channel gains across a bandwidth of 1 GHz for one of the channel realizations as shown in (b). (d) Channel gains across a bandwidth of 8 MHz for one of the channel realizations as shown in (b).

i.e, only 1/12 wavelength at 1.8 GHz. It is reasonable to assume unchanged channel gains during the period.

B. Inter-cell interference

We in this subsection show the inter-cell interference among UAV-UEs via a simulation. The simulation parameters are included in Table II. Briefly, we consider a rural scenario where 48 sectored cells, as illustrated in Fig. 3, were deployed. The BS heights were 35 m, the downtilts of the sector antennas were 8.5°, and the Inter-site distance (ISD) was 2 km. In each realization, 48 UAV-UEs were randomly generated in the 48 cells at the height of 60 m. For the large-scale fading, i.e., path loss and shadowing, we reproduce the measurement results obtained in [37]. Specifically, the PLE, standard deviation of the shadowing [dB] and the intercept point at 1 m are set as 2.1, 4.4 dB and 32.8 dB for the height of 60 m, respectively. For the characteristics of multipath components that account for small-scale fading, we reproduce channels that were observed in the ultra-wideband A2G channel measurements in [41]. Specifically, tapped-delay-line channels are statistically realized according to the procedure as specified in [43], [44].

The generated channels are illustrated in Fig. 2, where the power delay profile and the channel gain evolving across the frequency band are intended to be similar to that in [41]. Moreover, the considered bandwidth in this work is set as 9 MHz, i.e., half the maximum effective bandwidth of a LTE system. It can be observed from Fig. 2(d) that the channel gain is quite flat. Note that the discretized/blocked channel gains with 20 steps are finally applied.

The power control algorithm applied in the simulation was open loop power control (OLPC). Specifically, the transmitted power P_u in dBm is obtained as [45]

$$P_u = \min\{P_{\max}, P_0 + 10\log_{10}(M_{RB}) + \alpha PL\} \qquad (1)$$

where $P_{\max}$ is the configured maximum output power (which was 23 dBm[2]), PL is path loss, M_{RB} is the number of RBs allocated for this UE, α is the fractional power control compensated parameter, and P_0 is the power received at one RB if path loss is fully compensated. Note that P_0 and α were optimized by exhaustive searching (within [-90, -70] dBm and [0.5, 1] respectively) in the simulation scenario as illustrated in Fig. 3. Five hundred realizations were performed to obtain a distribution of the SINRs of individual UAVs. Fig. 4 illustrates the cumulative distribution functions (CDFs) of SINRs with UAVs equipped with omni-directional antennas, direction antennas of 60° HPBW and directional antennas of 30° HPBW, respectively. It can be observed from Fig. 4 that omni-directional antennas onboard UAVs can usually cause severe interference. Using directional antennas with HPBWs of 60° can improve the SINRs significantly, due to the directional radiation pattern suppressing interference. However, the improvement from 60°-HPBW antennas to 30°-HPBW antennas is much less than that from omni-directional to 60°-HPBW antennas. This means that using 60°-HPBW antennas could be a suitable choice considering the performance improvement and complexing increase. Nevertheless, interference can still be sometimes high for some UAV-UEs.

C. Packet scheduling for multiple UAV-UEs in one cell

We use both time-domain and frequency-domain packet scheduling for multiple UAV-UEs in the same cell. Conventionally in cellular networks, e.g. LTE, packet scheduling is achieved via the so-called *frequency domain packet scheduling (FDPS)* [47], [48] (note that time-domain is inherently considered in FDPS). The instantaneous channel conditions of UEs at all RBs in a cell are the inputs of FDPS, according to which different bandwidth portions are dynamically allocated to different UEs to better exploit the available frequency and user diversity, meanwhile fulfilling the uplink SC constraint. A well-known and commonly used approach is the proportional fair (PF)-FDPS that maximizes the long-term sum logarithmic utility of the system [48], [49]. Specifically, consider a cell with a set $\mathcal{K} = \{1, \cdots, K\}$ of UEs and a set $\mathcal{C} = \{1, \cdots C\}$

[2]According to the standard 3GPP TS 38.101-1 [46], the maximum transmission power of UEs operating at sub-6 GHz bands is 23 dBm. Currently, there are no standards dedicated to UAV-UEs. Therefore we use 23 dBm in this work.

Table II: Important parameters configured in the simulation.

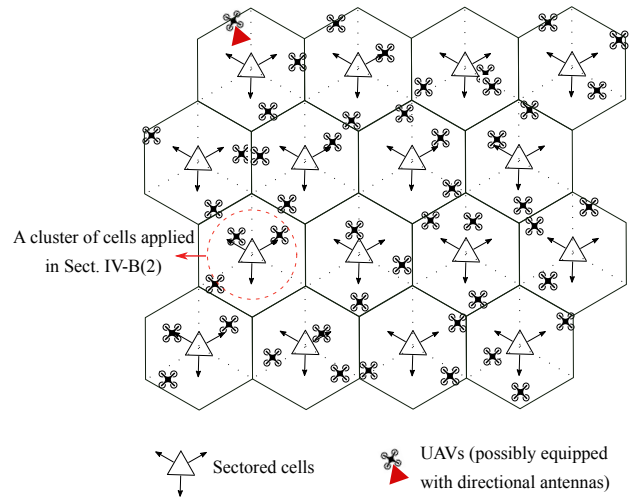| Main parameters applied in the simulation	
Network scale	48 cells
Cell type	Sectored hexagon
ISD	2 km
BS height	35 m
Sector antenna HPBWs	120° in azi.; 13° in ele.
Sector antenna downtilt	8.5°
UAV height	60 m
Maximum uplink power	23 dbm
Noise power density	-174 dBm/Hz
P_0	-81 dBm
α	0.9
PLE	2.1
Path loss at 1 m	32.8 dB
Std. of shadowing	4.4 dB
Tapped-delay-line channel	[41]

Fig. 3: An example realization of 48 UAVs located in the 48 sectored cells.
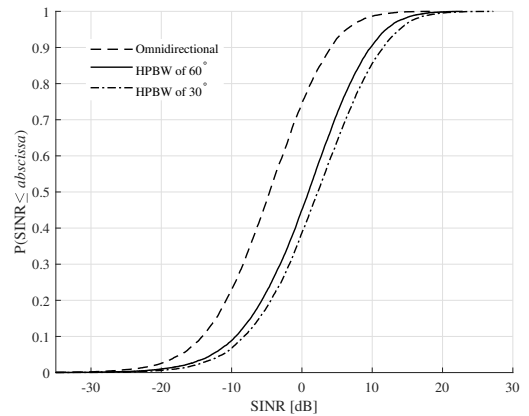

Fig. 4: SINR distributions using different antennas onboard UAVs.

of RBs, the cth RB at time t is allocated to the UE with index $\hat{k}_c(t)$ such that

$$\hat{k}_c(t) = \arg\max_k \quad r_k^c(t)/R_k(t) \tag{2}$$

where $r_k^c(t)$ indicates the data rate potentially achievable by the kth user on RB c at time t, and $R_k(t)$ is the historical average rate of the kth UE. In the focused communication scenario where all UAV-UEs are with close-to frequency-flat channels, r_k^c's of the kth UE tend to be similar across all the C RBs.[3] With SC constraint further considered e.g. as shown in [48], the PF-FDPS tends to allocate almost all RBs to the same UAV-UE. In other words, much less frequency diversity gain can be harvested for UAV-UEs compared to that of terrestrial UEs with frequency selective channels. Thus, in this work, we exploit time-domain PF to decide which UAV-UE or UAV-UEs to be active for transmission in the bursty-traffic mode in later Sect. IV-B. After that, power allocation is optimized.

III. PROPOSED POWER ALLOCATION ALGORITHMS

The main motivation is to maximize the sum SE of all UAV-UEs or maximize the minimum SE among all UAV-UEs. The first emphasizes the overall performance of the system, while the second emphasizes fairness among the UAV-UEs. A compromise between the two can be done by maximizing the sum SE of the system with individual quality of service (QoS) constraints considered for UAV-UEs. By leveraging the special channel properties of UAV-UEs, i.e., large coherent bandwidths and coherent times, the optimization can be realized in the frequency domain and/or the time domain. An intuitive example is that two UAV-UEs can transmit on the first and second half bandwidths, respectively, to avoid severe interference between them when both of them use the whole bandwidth simultaneously. This can be similarly applied in the time domain. However, with the number of UAV-UEs becoming much larger, the complexity of the problems increases fatally. Considering the constraint of SC uplink transmission further complicates the problems. In the sequel, we propose different algorithms and techniques in the frequency domain and/or the time domain to solve the problems, so that the performance of the uplink UAV communications can be enhanced.

A. Frequency-domain maximization of the minimum SE of UAV-UEs

As discussed in Sect. II-C, let us first consider the case where at most one UE is scheduled simultaneously in a cell. That is, at a transmision time interval (TTI) a set $\mathcal{N} = \{1, \cdots, N\}$ of cells are active each with one UAV-UE scheduled. In each cell, all the reserved bandwidth B is allocated to the scheduled UAV-UE and divided into $\mathcal{S} = \{1, \cdots, S\}$ segments. We denote the channel gain from the UAV-UE in the ith cell to the jth cell BS at the sth frequency block as G_{ijs}, and all the channel gains are contained in $\mathbf{G} = [G_{ijs}]$. Intuitively, G_{iis} is the gain of the serving link, whereas $G_{ijs}, i \neq j$ are that of interfering links. Note that G_{ijs} is attributed to the path loss, shadow fading, small-scale fading, and radiation patterns of

antennas. The power density of thermal noise is indicated by N_0, and the transmitted power of the ith UAV-UE on the sth bandwidth segment is denoted by p_{is}. Then the serving SINR γ_{is} of the ith UAV-UE on the sth bandwidth segment can be calculated as

$$\gamma_{is}(\mathbf{p}) = \frac{p_{is}G_{iis}}{N_0 B S^{-1} + \sum_{j \in \mathcal{N}, j \neq i} p_{js} G_{jis}}. \tag{3}$$

where $\mathbf{p} = [p_{is}], i \in \mathcal{N}, s \in \mathcal{S}$ is the compact notation of the power allocation for all the UAV-UEs. The achieved SE (bit/s/Hz) R_i of the ith UAV-UE is then calculated according to Shannon formula as

$$R_i(\mathbf{p}) = S^{-1} \sum_{s \in \mathcal{S}} R_{is}. \tag{4}$$

with

$$R_{is}(\mathbf{p}) = \log_2(1 + \gamma_{is}(\mathbf{p})). \tag{5}$$

The problem of maximizing the minimum SE of all UAV-UEs can be formulated as

$$
\begin{aligned}
\underset{\mathbf{p}}{\text{maximize}} \quad & \min_i R_i \\
\text{subject to} \quad & p_{i,\min} \leq p_i \leq p_{i,\max}, \quad \forall i \in \mathcal{N} \\
& p_i = \sum_{s \in \mathcal{S}} p_{is}, \qquad \forall i \in \mathcal{N}
\end{aligned}
\tag{6}
$$

where p_i is the total output power of the ith UAV-UE usually confined in a range from $p_{i,\min}$ (e.g., 0) to $p_{i,\max}$ (e.g., 23 dBm), and the objective is to find the optimal $\mathbf{p}^*$ solving the problem. Note that p_{is} of the ith UE can be dependent on s. The underlying reasoning is that this allows competing UAV-UEs transmitting on different bandwidth resources with different power densities to avoid severe interference so that the minimum SE can be increased. An intuitive case is that two neighboring edge-UEs are allowed to transmit on the first half B and the second half B, separately. Nevertheless, problem (6) omits the uplink SC constraint, i.e., the same power density must be applied for continuous RBs. We discuss first how to solve (6) and consider the SC constraint later. Problem (6) can be equivalently rewritten by introducing auxiliary variables b_i's and a_{is}'s as

$$
\begin{aligned}
\underset{\mathbf{p},[a_{is}],[b_i]}{\text{maximize}} \quad & \min_i b_i \\
\text{subject to} \quad & S^{-1} \log_2\{\prod_{s=1}^{S}(1 + a_{is})\} \geq b_i, \qquad \forall i \in \mathcal{N} \\
& \gamma_{is} \geq a_{is}, \qquad \forall i \in \mathcal{N}, \quad \forall s \in \mathcal{S} \\
& p_{i,\min} \leq p_i \leq p_{i,\max}, \qquad \forall i \in \mathcal{N} \\
& p_i = \sum_{s \in \mathcal{S}} p_{is}, \qquad \forall i \in \mathcal{N}
\end{aligned}
\tag{7}
$$

---

[3]They are not exactly the same because the interference may change at different RBs.

which is equivalently

$$\underset{\mathbf{p},[a_{is}],[b_i]}{\text{maximize}} \quad \min_i b_i$$

$$\text{subject to} \quad \frac{b_i}{\prod_{s=1}^{S}(1+a_{is})} \leq 1, \qquad \forall i$$

$$\frac{a_{is}N_0BS^{-1} + \sum_{j \neq i} a_{is}p_{js}G_{jis}}{p_{is}G_{iis}} \leq 1, \quad \forall i,s$$

$$p_{i,\min} \leq p_i \leq p_{i,\max}, \qquad \forall i$$

$$p_i = \sum_{s \in \mathcal{S}} p_{is}. \qquad \forall i$$

$$(8)$$

This is a non-convex problem. If $a_{is} \gg 1$ holds for all i and s, i.e., $\prod_{s=1}^{S}(1+a_{is})$ can be well approximated by $\prod_{s=1}^{S} a_{is}$, problem (8) is almost a GP-problem where a posynomial is minimized with upper bounded posynomial and/or equality monomial constraints [30], [50], [51]. However, interference in the UAV communications are generally significant. It is also possible that a UAV-UE may not transmit power at some bandwidth segments to avoid interference. Therefore, we resort to solving the problem via a series of GPs using the single condensation principle [30], [50]. In our case, the term $g_i(\mathbf{A}) = \prod_{s=1}^{S}(1+a_{is})$ is replaced by a monomial $h_i(\mathbf{A}) = \prod_{s=1}^{S} c_i s_{is}^{w_{is}}$, where matrix $\mathbf{A}$ contains all a_{is}, i.e. $\mathbf{A} = [a_{is}]$, and c_i and w_{is}'s are constants to be properly set. Problem (8) can then be solved according to Algorithm 1. It is essential that the h_i meets three requirements [30] to achieve convergence and feasibility of finally resulted power allocation, which include *i)* $h_i(\mathbf{A}) \leq g_i(\mathbf{A})$ for all $\mathbf{A}$. This is to guarantee the resulting power allocation always meets the original constraints. *ii)* $h_i(\mathbf{A}_0) = g_i(\mathbf{A}_0)$ at the condensation point $\mathbf{A}_0$. This guarantees the monotonicity of optimal values obtained in successive iterations. *iii)* $\nabla h_i(\mathbf{A}_0) = \nabla g_i(\mathbf{A}_0)$ at the condensation point. This is to make sure that after convergence, Karush–Kuhn–Tucker (KTT) conditions for the original problem are also met. *A major challenge of the condensation is that its complexity may increases exponentially with the number of UAVs* [30]. Therefore, we use a novel condensation whose complexity is linear, which can well cope with the massive UAV case. Specifically, we first consider a simple case for the condensation of $1 + a_i$, i.e., $S = 1$, that satisfies requirement *iii)*, it is easy to know that

$$w_i = \frac{a_{i,0}}{1+a_{i,0}}. \qquad (9)$$

To further meet requirement *ii)*, we have

$$c_i = (1+a_{i,0})a_{i,0}^{-w_i} \qquad (10)$$

and it is straightforward to check that the requirement *i)* is also met. Thus, for a general condensation of $g_i(\mathbf{A})$ at the approximation point $\mathbf{A}_0$, c_i's and w_{is}'s can be calculated as

$$w_{is} = \frac{a_{is,0}}{1+a_{is,0}},$$

$$c_i = g_i(\mathbf{A}_0)(\prod_{s=1}^{S} a_{is,0}^{w_{is}})^{-1}. \qquad (11)$$

Algorithm 1 Solving problem (8).

Input: A feasible power allocation $\mathbf{p}$ for initialization
Output: Optimized $\mathbf{p}^*$ that maximizes the minimum SE.

1: **Repeat:**
2: Calculate $\mathbf{A}_0$ according to the current power allocation $\mathbf{p}$, i.e., $\mathbf{A}_0 = [\gamma_{is}(\mathbf{p})]$.
3: Perform condensation at the current point $\mathbf{A}_0$, i.e., calculate c_i's and w_{is}'s at $\mathbf{A}_0$ according to (11).
4: Solve the GP problem with the condensation applied. The current power allocation $\mathbf{p}$ is updated as the newly optimized power allocation.
5: **Until** the power allocations obtained in two successive iterations change little, i.e., $||\mathbf{p}_{\text{now}} - \mathbf{p}_{\text{pre}}|| < \epsilon$ with ϵ being a pre-defined tolerance. The final optimized power allocation $\mathbf{p}^*$ is then chosen as the current power allocation.

Algorithm 2 A heuristic algorithm solving problem (8) with SC constraint.

Input: A feasible power allocation $\mathbf{p}$ for initialization
Output: Optimized $\mathbf{p}^*$ that maximizes the minimum SE while also fulfilling SC constraint.

1: Obtain $\mathbf{p}^*$ using Algorithm 1.
2: Allocate continuous frequency resources based on the SINRs achieved at $\mathbf{p}^*$ using Algorithm 3.
3: Perform Algorithm 1 again with the SC constraint considered to update $\mathbf{p}^*$.

It can be known that the complexity of the proposed condensation is linearly increasing with S, which is essential to make the SCA feasible for the uplink communications of a large number of UAVs.

Considering the uplink SC constraint: The power level of the same UE at different bandwidth segments obtained by Algorithm 1 can be arbitrarily different. This is applicable whenever the uplink SC constraint is no longer needed. Considering the SC constraint to maximize the minimum SE is NP-hard [48]. Thus we proposed a heuristic Algorithm 2 for this purpose based on Algorithm 1. The proposed algorithm mainly includes three steps. *i)* Obtain the first power allocation $\mathbf{p}^*$ using Algorithm 1 without SC constraint. *ii)* Allocate continuous frequency resources for UAV-UEs according to the result obtained in *i)*. *iii)* Perform Algorithm 1 again considering the SC constraint as posed by step *ii)*. That is, for each UAV, the power density on the allocated continuous segments is kept the same, and the power density of non-allocated segments is zero.

The heuristic part (step *ii)*) of Algorithm 2 is described as Algorithm 3. The purpose is to find continuous bandwidth segments of each UE with powers that change as little as possible. *Here, we exploit an important characteristic of the A2G channel. That is, the channels are close to frequency-flat, as shown in Fig. 2(d). Therefore, we can reorder the columns of $\mathbf{p}^*$ obtained in step i) while keeping the same optimization performance, which is essentially not possible*
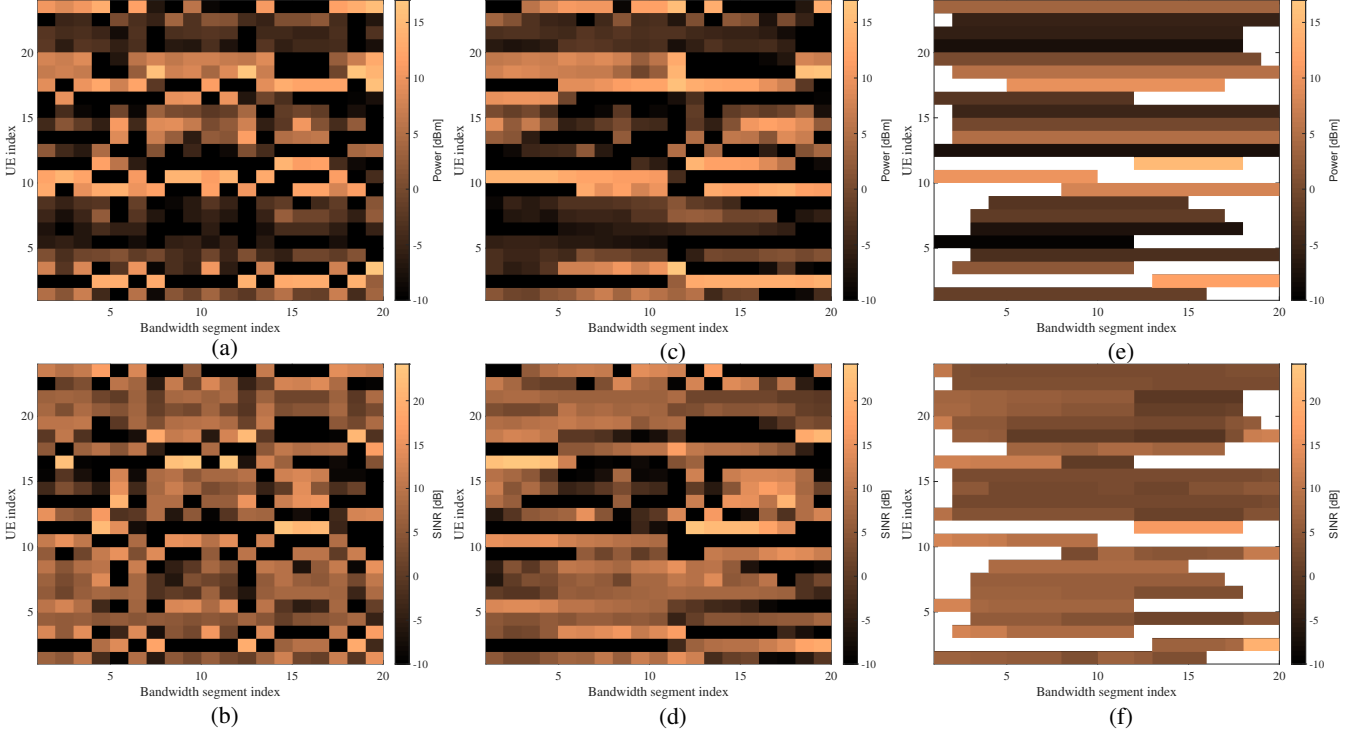
Fig. 5: An example application of Algorithm 2. (a) Power allocation obtained using Algorithm 1. (b) The corresponding SINR matrix. (c) Reordered power allocation in Algorithm 3. (d) The corresponding reordered SINR matrix. (e) Final power allocation with SC constraint considered. (f) The corresponding SINR matrix of SC transmission.

for terrestrial UEs. Intuitively, if there exist two or more UAV-UEs causing significant interference to each other on the same frequency resource, they probably will use different resources, and their SINRs on some segments could be very low. To increase the minimum SE as possible, it is necessary to identify and put emphasis on this kind of UEs. We thus exploit the SINR matrix to reorder columns. The first step in Algorithm 3 is to find the UE with index i that has the minimum γ_{is} in the SINR matrix $\mathbf{\Gamma}(\mathbf{p}^*) = [\gamma_{is}]$. Then the SINR matrix and power matrix are updated by rearranging the columns according to descending/ascending order of the S SINRs of the ith UAV-UE on the S bandwidth segments. This is trying to smooth the SINR change (and power change) at neighboring bandwidth segments. Finally, for each UE, expanding continuous frequency resources starting with the bandwidth segment having the largest SINR till the summed rate on these bandwidth segments is larger than a pre-defined threshold of the original overall summed rate on all S segments. Fig. 5 illustrates an example application of Algorithm 2. In this example, 24 cells are active each with a UAV-UE. Bandwidth B is divided into $S = 20$ segments. It can be clearly observed from Fig. 5(c) or (d) that UEs #2 and #10 are using interleaved bandwidth segments, which means that they cause severe interference to each other if transmitting on the same frequency resource, e.g. when $S = 1$. The finally maximized minimum equivalent SINR (i.e., $2^{SE}-1$) obtained using Algorithm 2 in this case is 3.2 dB. As a comparison, the maximized minimum equivalent SINR obtained using Algorithm 1 without considering SC constraint, as shown in Fig. 5(b), is 4.9 dB due to more freedom in power allocation.

Algorithm 3 A heuristic algorithm for SC bandwidth allocation.

Input: SINR matrix $\mathbf{\Gamma} = [\gamma_{is}]$ achieved at final $\mathbf{p}^*$ using Algorithm 1 without considering SC constraint.

Output: Bandwidth allocation fulfiling SC constraint.

1: Find the index i of the UE having the minimum SINR, i.e., $(i, s) = \arg\min_{j,v} \gamma_{jv}$.
2: Update $\mathbf{\Gamma}$ by rearranging its columns according to descending order of the SINRs at S bandwidth segments of the ith UE.
3: For each UE, start with its bandwidth segment with largest SINR and expand continuously to neighboring ones till the summed rate exceeds a pre-defined proportion η of the original overall rate.

Whereas when using the whole bandwidth, i.e. $S = 1$, for SC transmission, the maximized minimum equivalent SINR is only -3.6 dB. This significant gain of around 7 dB in SINR illustrates the effectiveness of the proposed algorithm.

B. Time-domain maximization of the minimum SE of UAV-UEs

This is an algorithm proposed for the case where the UAV-UEs are allowed to transmit for a certain period, e.g., a set $\mathcal{T} = \{1, \cdots, T\}$ of TTIs, which is still within the coherent time of the channels. In each TTI, we assume a UAV-UE is using the whole B with the same power density to not complicate the expression without losing the essence. The problem can then

be formulated as

$$\underset{\mathbf{p}}{\text{maximize}} \quad \min_i R_i$$
$$\text{subject to} \quad p_{i,\min} \leq p_{it} \leq p_{i,\max}, \forall i \in \mathcal{N}, \forall t \in \mathcal{T} \tag{12}$$

where $\mathbf{p} = [p_{it}]$ with p_{it} indicating the output power of the ith UAV-UE at the tth TTI. Moreover, R_i is also modified as

$$R_i(\mathbf{p}) = T^{-1} \sum_{t \in \mathcal{T}} \log_2(1 + \gamma_{it}) \tag{13}$$

with

$$\gamma_{it}(\mathbf{p}) = \frac{p_{it} G_{ii}}{N_0 B + \sum_{j \in \mathcal{N}, j \neq i} p_{jt} G_{ji}}. \tag{14}$$

This problem, with a similar format to (8), can be solved essentially almost the same as described in Algorithm 1. *Nevertheless, it is not exactly the same to* (8). One reason is that power levels of a UAV-UE at different TTIs can be arbitrarily different, i.e., the SC constraint is naturally met. The other reason is that in (8), since a UAV-UE can use less bandwidth, its maximum power density is higher than that achieved in (12), which may result in different performances. They are also the reasons that we discuss time-domain and frequency-domain algorithms separately.

C. Frequency-domain maximization of the sum SE of UAV-UEs

Besides maximizing the minimum SE of UAVs in the system, another principle can be to maximize the overall SE of all UAVs in the system, depending on the application scenarios. Based on the notations as described in Sect. III-A, we formulate the problem as

$$\underset{\mathbf{p}}{\text{maximize}} \quad \sum_{i=1}^{N} R_i$$
$$\text{subject to} \quad p_{i,\min} \leq p_i \leq p_{i,\max}, \forall i \in \mathcal{N}$$
$$p_i = \sum_{s \in \mathcal{S}} p_{is}, \forall i \in \mathcal{N} \tag{15}$$
$$R_i \geq R_{i,\min}, \forall i \in \mathcal{N}$$

where the last line in (15) is the QoS constraints. We propose Algorithm 4 to solve (15) with the SC constraint also considered, which can be the most complicated case. The key is to find an initial feasible SC power allocation (may not exist) that meets the QoS constraint, which must be based on the algorithm proposed in Sect. III-A. We do not redundantly write algorithms for other easier cases. For example, without SC constraint, the step 1 in Algorithm 4 can be modified as to exploit Algorithm 1 to find an initial feasible power allocation, and the SC constraint is also removed from step 3.

D. Time-domain maximization of the sum SE of UAV-UEs

This can be formulated from Sect. III-B, as similarly done from Sect. III-A to Sect. III-C. We thus omit the detailed formulas.

E. Scheduling and power control for multiple UAV-UEs

Multiple UAV-UEs in a cell, e.g. a set $\mathcal{K}_i = \{1, \cdots, K_i\}$ of UEs with the K_i highest time-domain PF priorities in

---

Algorithm 4 Solving problem (15) considering SC constraint.

Output: Optimized $\mathbf{p}^*$ that maximizes the sum SE fulfilling both QoS and SC constraints.

1: Apply Algorithm 2 to obtain the uplink SC bandwidth allocation and the maximized-minimum QoS.
2: **if** the achieved QoS can meet the constraint in (15) **then**
3:    Use the power allocation obtained in 1 as a feasible initialization, and perform a series of GPs considering SC bandwidth allocation till convergence.
4: **else**
5:    No feasible solution.
6: **end if**

---

the ith cell, may be allowed to transmit simultaneously. The methodology is essentially similar to what we have discussed for single-UE cases. For example, to maximize the minimum SE of all UAV-UEs in the network, the problem can be formatted similarly to (6) as

$$\underset{\mathbf{p}}{\text{maximize}} \quad \min_{i,k_i} R_{i,k_i}$$
$$\text{subject to} \quad p_{i,k_i,\min} \leq p_{i,k_i} \leq p_{i,k_i,\max}, \quad \forall i, k_i \tag{16}$$
$$p_{i,k_i} = \sum_{s \in \mathcal{S}} p_{i,k_i,s}, \quad \forall i, k_i$$

with the SE of the k_ith UE in the ith cell modified as

$$R_{i,k_i}(\mathbf{p}) = K_i^{-1} S^{-1} \sum_{s \in \mathcal{S}} R_{i,k_i,s}. \tag{17}$$

because in total K_i UAV-UEs share the frequency resources in the ith cell. With the SC constraint further considered, one can exploit Algorithm 2 to conduct packet scheduling and power allocation for individual UEs. An additional consideration is that UEs in the same cell have to use orthogonal bandwidth segments unless non-orthogonal multiple access (NOMA) technique is applied.

IV. SIMULATION AND DISCUSSIONS

In this section, we demonstrate the performances of the different algorithms proposed in Sect. III via extensive simulations. Full-buffer mode and bursty-traffic mode are considered in Sect. IV-A and Sect. IV-B, respectively. To ease the description of the proposed algorithms, the abbreviations as shown in Table III are applied. We use e.g. "FD SC Max-Min" to denote *frequency domain maximization of the minimum SE considering SC constraint*. The abbreviation style is similarly applied to other algorithms.

A. full-buffer mode

1) The case of single UE per cell:

In this subsection, we focus on the full-buffer uplink transmission mode, where UAV-UEs are assumed to constantly transmit uplink data. In the simulation, a network with 48 sectored cells as illustrated in Fig. 3 is applied. Important simulation parameters are the same as included in Table II in Sect. II-B. We assume that an array consisting of six antennas

Table III: Algorithms utilized in the simulation.

Abbreviation	Referring to
OLPC	(1) in Sect. II-B
FD/TD Max-Sum w/o QoS ($S=1/T=1$)	Sect. III-C
FD/TD Max-Min ($S=1/T=1$)	Algorithm 1 in Sect. III-A
FD Max-Min ($S=20$)	Algorithm 1 in Sect. III-A
FD SC Max-Min ($S=20$)	Algorithm 2 in Sect. III-A
FD SC Max-Sum with QoS ($S=20$)	Algorithm 4 in Sect. III-C
TD Max-Min ($T=20$)	Sect. III-B
TD Max-Sum with QoS ($T=20$)	Sect. III-D

FD: Frequency domain; TD: Time domain; Max-Sum: Maximization of the sum SE; Max-Min: Maximization of the minimum SE; QoS: QoS constraint; SC: Single carrier; S: Segment number in frequency domain; T: TTI number.
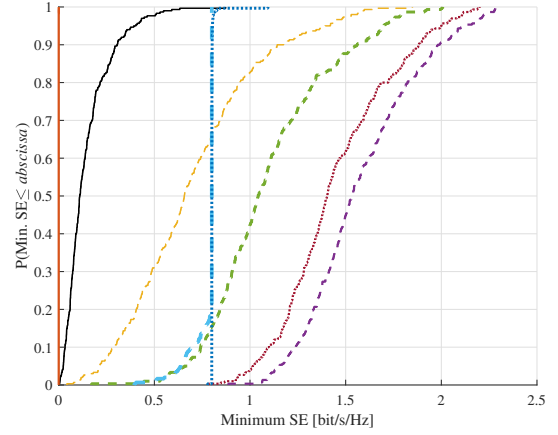
Table IV: Performance gains (in percentage) for the H-th percentile SEs of all UAV-UEs in the full buffer mode compared to OLPC. The top three best algorithms are bolded.

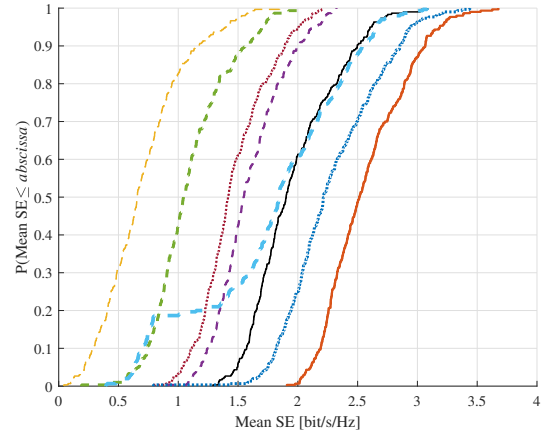| Algorithms \ H	10	20	50	100
FD/TD Max-Sum w/o QoS. ($S=1/T=1$)	-100%	-100%	**44%**	**16%**
FD/TD Max-Min ($S=1/T=1$)	-18%	-33%	-59%	-81%
FD Max-Min ($S=20$)	**265%**	**123%**	**-5%**	-76%
FD SC Max-Min ($S=20$)	119%	**38%**	-36%	-80%
FD SC Max-Sum with QoS. ($S=20$)	99%	32%	-49%	**1%**
TD Max-Min ($T=20$)	**225%**	**102%**	-12%	-77%
TD Max-Sum with QoS. ($T=20$)	**138%**	35%	**7%**	**4%**

with 60° HPBWs is onboard the UAV [13], and the best directional antenna is switched on for the uplink communication. The percentage of active cells ranges from 0.5 to 1. That is, in each realization, a random portion of the 48 cells are active with a UAV-UE in full-buffer mode transmission. Totally 300 realizations, each with random locations of UAVs, are performed. The first consideration is to obtain the statistical performance of the proposed algorithms. The second is to include the effect of mobility of UAVs which can statistically lead to randomized locations of UAVs in each cell.

Fig. 6 illustrates the CDFs of SEs obtained using the proposed algorithms as summarized in Table III.[4] Specifically, Fig. 6(a) illustrates the CDFs of the minimum SEs achieved in individual realizations, Fig. 6(b) illustrates the CDFs of the mean SEs obtained in individual realizations, and in Fig. 6(c) the CDFs of SEs of all UAV-UEs in all realizations are presented. In the OLPC algorithm, UAV-UEs are transmitting on the whole reserved bandwidth according to (1) with the optimized P_0 and α as shown in Table II. For other algorithms, Max-Sum is conducted without QoS constraint. In the frequency domain, three different Max-Min algorithms are performed which include FD Max-Min ($S = 1$), FD Max-Min ($S = 20$) and FD SC Max-Min ($S = 20$). Moreover, FD SC Max-Sum ($S = 20$) is also applied with QoS constraint set as 0.8 bit/s/Hz for all UAV-UEs. Similarly in the time domain, TD Max-Min ($T = 20$) and TD Max-Sum ($T = 20$) with QoS constraint as 0.8 bit/s/Hz are conducted. Table IV summarizes
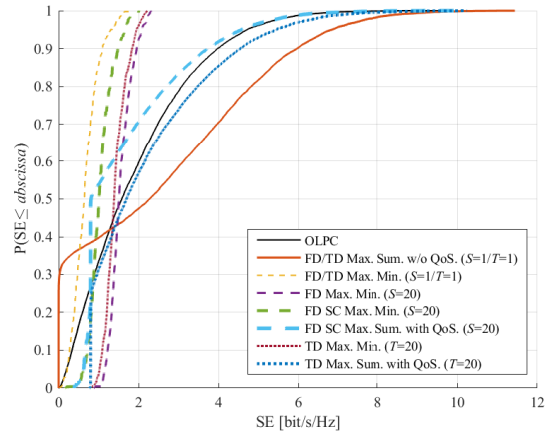
[4]Although the closed loop power control (CLPC) [52], [53] could have better performance for cell-edge UEs, it has many more parameters to be tuned compared to the OLPC. Moreover, it is still a non-optimized power control scheme. Therefore, we choose the tuned OLPC in the simulation as the non-optimized baseline for comparison.

(a)

(b)

——	OLPC
——	FD/TD Max. Sum. w/o QoS. ($S=1/T=1$)
- - -	FD/TD Max. Min. ($S=1/T=1$)
- - -	FD Max. Min. ($S=20$)
- - -	FD SC Max. Min. ($S=20$)
- - -	FD SC Max. Sum. with QoS. ($S=20$)
······	TD Max. Min. ($T=20$)
······	TD Max. Sum. with QoS. ($T=20$)

(c)

Fig. 6: CDFs of SEs of UAVs in full-buffer mode. (a) Minimum SEs obtained in individual realizations. (b) Mean SEs obtained in individual realizations. (c) SEs of all UAV-UEs in all realizations.

the performance gains of these algorithms applied in the full-buffer mode for different groups of UAV-UEs compared to that of OLPC. According to the three subfigures of Fig. 6 and Table IV, we have the following observations and findings.

- The Max-Min algorithms can achieve better minimum SEs compared to that of OLPC and Max-Sum without QoS constraint. Especially, the minimum SE of Max-Sum without QoS constraint is almost always zero, which means that in the interference dominant scenario, there are always UE(s) being sacrificed to maximize the sum SE. Moreover, it can be observed that with a larger S or no SC constraint, FD Max-Min can achieve a larger minimum SE. This is reasonable since a larger S and/or no SC constraint can provide more freedom for UAV-UEs to avoid severe interference by transmitting on interleaved bandwidth segments. Furthermore, we can observe that the performance of TD Max-Min ($T = 20$) is close to that of FD Max-Min ($S = 20$) regarding the achieved minimum SE. This is understandable because the SC constraint is not a concern in the time domain while still keeping the similar freedom of avoiding severe interference by transmitting at interleaved times. Thus, TD Max-Min is considered a good option. Nevertheless, the power density in FD Max-Min can be higher which is advantageous for edge UEs, so that the performance of TD Max-Min is slightly lower than that of FD Max-Min

- Although the various TD/FD Max-Min algorithms can achieve better minimum SEs, they have less mean SEs compared to that of OLPC. The reason is that in the Max-Min algorithms, all the UAV-UEs in a realization are with the same SE, as we can observe that the curves of Max-Min algorithms in Figs. 6(a)-(c) are the same. This is also easy to be verified by contradiction as follows. Assume that there are one or several UEs with higher SEs, then their transmitting powers can be decreased to increase the minimum SE until all UAV-UEs have the same SE. Therefore, the SEs of UEs in good conditions are limited leading to smaller mean SE. In addition, it is straightforward that the Max-Sum without QoS constraint can achieve the best mean SE.

- Compared to OLPC, Max-Min algorithms are favorable to UEs in bad conditions however limit the SEs of UEs in good conditions; whereas the Max-Sum without QoS constraint sacrifices the UEs in bad conditions. By introducing QoS constraints into Max-Sum, the compromise can be tuned. For example, it can be observed from Fig. 6(a) that the minimum SEs of FD SC Max-Sum with QoS constraint and TD Max-Sum with QoS constraint are realized as 0.8 bit/s/Hz if there exist feasible solutions, otherwise the original Max-Min SEs are kept. It can be observed from Fig. 6(b) that the mean SEs are increased compared to that of the corresponding Max-Min algorithms. Moreover in Fig. 6(c), it can be observed that the SEs of UEs in bad conditions (e.g., UEs with SEs below the 20th percentile) are guaranteed, and the SEs of other UEs in better conditions are not limited too much either. It is worth noting that the TD Max-Sum with QoS
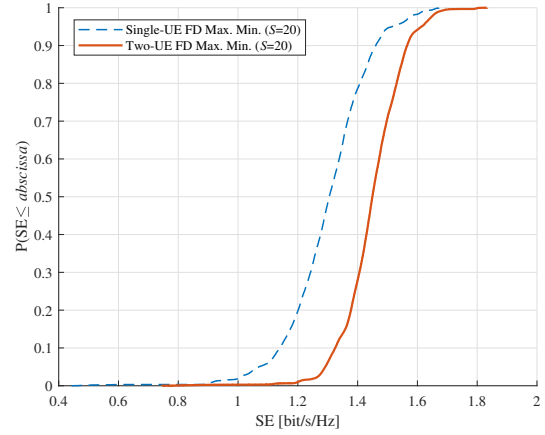

Fig. 7: CDFs of SEs of UAV-UEs obtained in the two-UE scheduling and single-UE scheduling in the full-buffer mode.

constraint herein can achieve overall better performance for both types of UEs compared to the OLPC algorithm.

2) The case of multiple UEs per cell:

As discussed in Sect. III-E, it is possible that multiple UAV-UEs can be scheduled in each cell. We consider herein a simple case, i.e. scheduling two UEs per cell in the full-buffer mode. All 48 cells are active, and the FD Max-Min algorithm with $S = 20$ is utilized. Fig. 7 illustrates the SEs of two-UE scheduling and the SEs of single-UE scheduling. It can be observed that the performance of two-UE scheduling is better than that of the single-UE scheduling. This is due to that by scheduling more UAVs, each UAV tends to use less bandwidth compared to that of single-UE scheduling. With the same allowed maximum transmit power, a higher maximum power density tends to be achieved in multiple-UE scheduling. For those UAVs with large path loss, i.e. power limited UAVs, higher power density is favorable for them to increase their SEs. This shows the potential of multiple-UE scheduling. In the bursty-traffic mode in the sequel, we still focus on the single UE scheduling.

B. bursty-traffic mode

In this subsection, we focus on the bursty-traffic mode, where each UAV-UE is assumed to transmit a packet of a certain size. The same network topology as described in Table II for the full-buffer mode is still applied herein for the bursty-traffic mode. Differently, UAV-UEs in the bursty-traffic mode are assumed to enter the network according to a Poisson distribution with an arrival rate λ as 2.5 UE/s/cell. All active UAV-UEs transmit 4 Mb data and leave the network once the transmission is finished. Additional parameters configured for the bursty-traffic mode are included in Table V. Furthermore, in the full-buffer simulation as discussed before, it is clear that we assume the algorithm or the computing center knows the information of the channel gains among all UAV-BS pairs, i.e. **G**, so that all the UAV-UEs can be optimized jointly. We denote it as "centralized application of algorithms", which may require considerable resources for UAV-UEs to perform

Table V: Additional parameters applied together with Table II for the bursty-traffic mode.

Main additional parameters for bursty-traffic mode	
Bandwidth B	9 MHz
Arrive rate λ of UAV-UEs	2.5 UE/s/cell
Packet size	4 Mb
Updating time interval	0.02 s
Simulation time	10 s

Table VI: Performance gains (in percentage) for the H-th percentile SEs of all UAV-UEs in the bursty traffic mode compared to OLPC. The top three best algorithms are bolded.

Algorithms \ H	10	20	50	100
FD/TD Max-Sum w/o QoS. (S/T=1)	**66%**	**60%**	**79%**	**85%**
FD SC Max-Min (S=20)	-37%	-50%	-60%	-77%
FD SC Max-Sum with QoS. (S=20)	-22%	-33%	-44%	**18%**
TD Max-Min (T=20)	**22%**	**2%**	**-21%**	-57%
TD Max-Sum with QoS. (T=20)	**83%**	**58%**	**32%**	**73%**

channel estimation and feedback the estimated channel information to the computing center. It is also possible to "de-centralize" the algorithm, e.g., that the optimizations are done for individual groups of UAV-UEs. For the bursty-traffic mode, we will discuss both centralized and de-centralized applications of algorithms in the sequel.

1) Centralized application of algorithms:

Fig. 8 illustrates the CDFs of SEs of UAV-UEs for different algorithms applied.[5] Specifically, the SE R_{bursty} of a UAV-UE in the bursty-traffic mode is calculated as

$$R_{\text{bursty}} = \frac{DataSize}{B(t_{\text{out}} - t_{\text{in}})} \tag{18}$$

where t_{in} and t_{out} are the time instants when the UE enters into and leaves the system, respectively, and $DataSize$ [bit] is the total amount of data transmitted by the UAV in the period from t_{in} to t_{out}. Moreover, the first 1.6 seconds of the system is not considered to exclude the "warming-up" stage. Fig. 8 provides the following insights.

- It is interesting to observe from Fig. 8 that in the bursty-traffic mode FD SC Max-Min and FD SC Max-Sum with QoS have smaller performances, i.e. R_{bursty} in (18), for all UAV-UEs than that of OLPC, although in the full-buffer mode they can achieve larger minimum SEs compared to that of OLPC. This is because the SEs of UAV-UEs in better channel conditions are limited to maximize the minimum SE or to meet the QoS constraint in each updating time interval. In other words, the mean (or sum) SE of UAV-UEs is decreased in an updating interval, as indicated in Fig. 6(b). Consequently, UAV-UEs in relatively good channel conditions stay in the system for a longer time compared to the case, e.g., in the Max-Sum without QoS constraint, where they can transmit at much higher rates. Moreover, since these UAV-UEs in relatively good conditions tend to be scheduled with higher priorities compared to those UAV-UEs in relatively bad channel conditions, the average SEs of UAV-UEs in bad channel conditions are also decreased due to longer inactive periods, although when they are active they indeed have higher minimum SEs, finally leading to smaller averaged SEs of all UAV-UEs in the bursty mode. This is similarly true for observing that TD-based

algorithms have better performance than that of their corresponding FD algorithms, e.g. from FD SC Max-Min to TD Max-Min, and for that TD/FD Max-Sum with QoS have better performances than TD/FD Max-Min in the simulation case herein.

- However, it is not necessarily that the larger the sum (or mean) SEs in individual updating time intervals are, the better the overall performance is. For example, comparing the curves of TD Max-Sum with QoS and Max-Sum without QoS, it can be observed that TD Max-Sum with QoS has better performance for UAV-UEs at lower percentiles, although Max-Sum without QoS indeed can achieve largest sum SE at each updating time interval. This is because in each updating time interval of Max-Sum without QoS constant, a certain number of UEs are almost muted with zero rates, as indicated in Fig. 6(c). This means that a SE balance between UAV-UEs in bad and good channel conditions in each updating time interval must be properly tuned to achieve a good system performance in the bursty-traffic mode, especially when the QoSs or SEs of UEs at lower percentiles are key evaluation metrics.

Table VI summarizes the performance gains of the algorithms applied in the bursty-traffic mode for different groups of UAV-UEs compared to that of OLPC. It can be seen that TD Max-Sum with QoS is a good algorithm with the best edge UE performance and still not bad overall performance. By tuning the QoS constraints, it is possible to achieve an optimized balance between UAV-UEs in bad and good channel conditions for pre-defined key evaluation metrics.

2) Decentralized (locally centralized) application of algorithms:

We also evaluate the performances of the algorithms when applying them separately to clusters of cells in the network. That is, the whole network is divided into several clusters of cells, and the algorithms are applied for each of these cells without considering the existence of other clusters in each updating time interval[6]. After optimizing the resource and power allocation of each cluster, the performance of the whole network is evaluated by combining all clusters.

---

[5]It can be seen in Table IV that Max-Min (S=1/T=1) has worse performances for all groups of UAV-UEs. Also considering that the uplink SC constraint is practically required, we thus omit Max-Min (S=1/T=1) and FD Max-Min (S=20) in the simulation of bursty-traffic mode.

[6]Note that they are different from the so-called distributed algorithms where the master problems are decomposed into several subproblems that are solved locally and synchronized through message-passing [54]. The results are different from that achieved in the centralized or distributed algorithms. Although how to realize distributed algorithms is not addressed in this paper, it is an interesting future work since the overhead can be reduced significantly compared to that of the centralized algorithms.
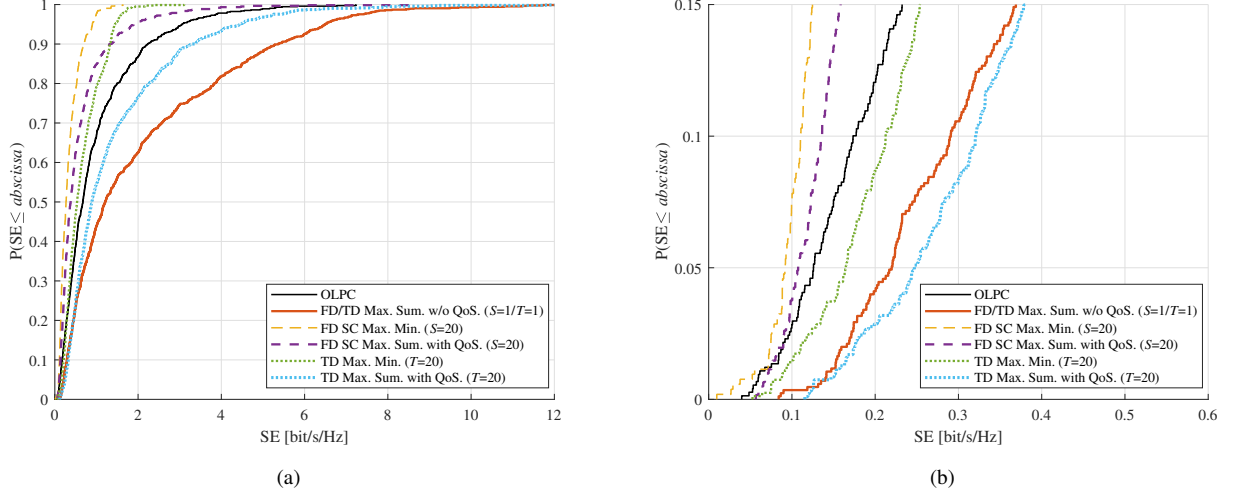
Fig. 8: Performance of different algorithms applied in the bursty-traffic mode. (a) CDFs of SEs of all individual UAV-UEs (b) Zoomed figure.
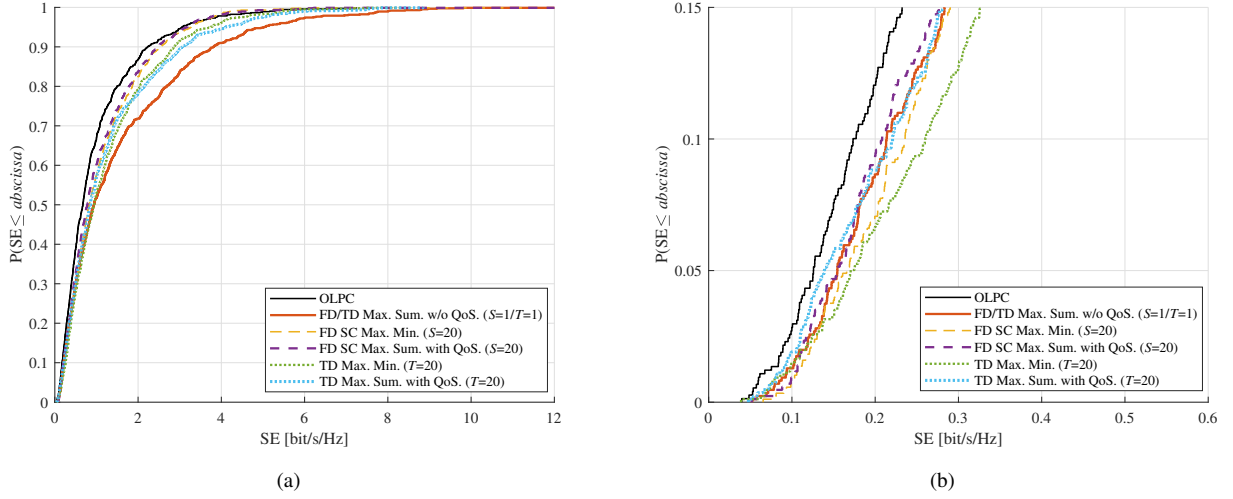

Fig. 9: Performance of different algorithms cluster-wise applied in the bursty-traffic mode. (a) CDFs of SEs of all UAV-UEs. (b) Zoomed figure.

The main reasons to do so include that *i)* The centralized way requires channel state information among all UEs and all sector cells, which is probably practically challenging and consumes additional resources for signaling; *ii)* Giving too much fairness among all UAV-UEs may finally degrade the overall performance since the UEs with relatively good channel conditions may be also limited; *iii)* Although a UAV-UE may cause interference to many cells, it is still true that the badly affected ones are cells relatively close to this UAV-UE in terms of distance and beam direction. In the simulation considered herein where individual UAV-UEs are assumed to use the best beam with a 60° of HPBW, each of three co-site sectored cells is grouped as a cluster as illustrated in Fig. 3, i.e., the whole network with 48 sector cells is divided into 16 clusters.

Fig. 9 illustrates the CDFs of the SEs of all UAV-UEs for different algorithms applied cluster-wise. It is interesting to

find that all the proposed algorithms have better performances compared to that of OLPC. Specially, FD SC Max-Min, FD SC Max-Sum with QoS and TD Max-Min are improved significantly compared to that as illustrated in Fig. 8. This is because fairness in each updating time interval is decreased which leads to a larger sum SE hence improving the final bursty performance. However, the performances of TD Max-Sum with QoS and Max-Sum without QoS decrease slightly compared to their centralized versions as shown in Fig. 8. The reason is that the centralized TD Max-Sum with QoS and Max-Sum without QoS can already achieve relatively good performances for both cell-edge and cell-center UAV-UEs, i.e., the fairness problem is not that severe as in, e.g., FD SC Max-Min, and decentralized applications of them instead decreases the performance since the UAV-UEs were not jointly optimized.

C. Overall discussions

Based on the extensive simulations in both full-buffer mode and bursty-traffic mode conducted for the proposed algorithms, we would like to summarize several points as follows.

- The proposed algorithms in the frequency domain and/or time domain can obtain the optimal or suboptimal resource and power allocations for UAV-UEs subject to certain constraints. Generally, time domain algorithms can achieve better performances, since SC constraint has to be considered when applying frequency domain algorithms. However, whenever the SC constraint is no longer required, frequency domain algorithms are better choices than the time domain algorithms, since higher power densities can be achieved.

- In the full-buffer mode which emulates high traffic load, algorithms that maximize the minimum SE can have the best minimum SE, whereas the SEs of UAV-UEs in good conditions, e.g. cell-center UAV-UEs, may be limited significantly. Maximizing the sum SE without considering QoS constraints can achieve the best sum SE. However, the SEs of some UAV-UEs can be always close to zero. Nevertheless, maximizing the sum SE considering QoS constraints is a compromise for both cell-edge and cell-center UAV-UEs. Moreover, it is possible to achieve an optimized value for the target key performance indicator by properly tuning the QoS constraint for different service scenarios.

- The performance of UAV-UEs in the bursty-traffic mode is different from that in the full-buffer mode. For example, it is not necessarily that the algorithm that maximizes the minimum SE in each updating time interval can achieve better averaged SEs for lower-percentile UAV-UEs. Overall, performances of all UAV-UEs depend on both the minimum SE and sum SE achieved in each updating time interval. The algorithm that maximized the sum SE in TD with a certain QoS constraint can be considered the best option for bursty-traffic mode transmission. It is worth noting that the centralized algorithms need to know all channel gains and require signaling to the central computation unit. The complexity of optimization also increases polynomially with the number of UAV-UEs. To decrease the signaling and computation load, decentralized application of algorithms could be a practical solution. The performance of decentralized frequency-domain algorithms is found to be increased, although they are still lower than that of the centralized TD maximization of sum SE with QoS constraints. Nevertheless, if the time domain algorithm cannot be done, e.g. due to the short updating time interval of the system, decentralized frequency domain algorithms can be good options.

V. Conclusions

In this contribution, different power allocation algorithms have been proposed for the uplink communications of a massive number of cellular-connected unmanned aerial vehicles (UAVs). Generally, the time-domain maximization of sum spectrum efficiency (SE) with a properly tuned quality of service (QoS) constraint works satisfactorily for UAVs in both high and medium/low traffic conditions. Other algorithms may emphasize different groups of UAV-UEs. Moreover, scheduling multiple UAVs are favorable for power-limited UAVs as the maximum power density can be increased. Cluster-wise applications, with lower computation and signaling loads, can also increase the performance of frequency domain algorithms. Future work can investigate joint optimization of scheduling and power allocation for multi-cell multi-UAVs. Moreover, since UAV engines usually consume a lot of energy, optimizing the flight trajectories of UAVs is also an important aspect to be (jointly) considered.

References

[1] B. Alzahrani, O. S. Oubbati, A. Barnawi, M. Atiquzzaman, and D. Alghazzawi, "UAV assistance paradigm: State-of-the-art in applications and challenges," *Journal of Network and Computer Applications*, vol. 166, p. 102706, 2020.

[2] N. Babu, C. B. Papadias, and P. Popovski, "Energy-efficient 3-D deployment of aerial access points in a UAV communication system," *IEEE Communications Letters*, vol. 24, no. 12, pp. 2883–2887, 2020.

[3] Y. Liu, K. Liu, J. Han, L. Zhu, Z. Xiao, and X. G. Xia, "Resource allocation and 3-D placement for UAV-enabled energy-efficient IoT communications," *IEEE Internet of Things Journal*, vol. 8, no. 3, pp. 1322–1333, 2021.

[4] L. Zhu, J. Zhang, Z. Xiao, X. Cao, X. G. Xia, and R. Schober, "Millimeter-wave full-duplex UAV relay: Joint positioning, beamforming, and power control," *IEEE Journal on Selected Areas in Communications*, vol. 38, no. 9, pp. 2057–2073, 2020.

[5] O. S. Oubbati, M. Atiquzzaman, A. Baz, H. Alhakami, and J. Ben-Othman, "Dispatch of UAVs for urban vehicular networks: A deep reinforcement learning approach," *IEEE Transactions on Vehicular Technology*, vol. 70, no. 12, pp. 13 174–13 189, 2021.

[6] S. Hayat, E. Yanmaz, and R. Muzaffar, "Survey on unmanned aerial vehicle networks for civil applications: A communications viewpoint," *IEEE Commun. Surveys Tuts.*, vol. 18, no. 4, pp. 2624–2661, 2016.

[7] N. Kumar, D. Puthal, T. Theocharides, and S. P. Mohanty, "Unmanned aerial vehicles in consumer applications: New applications in current and future smart environments," *IEEE Consum. Electron. Mag.*, vol. 8, no. 3, pp. 66–67, 2019.

[8] Y. Zeng, J. Lyu, and R. Zhang, "Cellular-connected UAV: Potential, challenges, and promising technologies," *IEEE Wireless Communications*, vol. 26, no. 1, pp. 120–127, February 2019.

[9] Y. Zeng, Q. Wu, and R. Zhang, "Accessing from the sky: A tutorial on UAV communications for 5G and beyond," *Proceedings of the IEEE*, vol. 107, no. 12, pp. 2327–2375, 2019.

[10] G. Geraci, A. Garcia-Rodriguez, L. Galati Giordano, D. López-Pérez, and E. Björnson, "Understanding UAV cellular communications: From existing networks to massive MIMO," *IEEE Access*, vol. 6, pp. 67 853–67 865, 2018.

[11] A. Garcia-Rodriguez, G. Geraci, D. Lopez-Perez, L. G. Giordano, M. Ding, and E. Bjornson, "The essential guide to realizing 5G-connected UAVs with massive MIMO," *IEEE Communications Magazine*, vol. 57, no. 12, pp. 84–90, 2019.

[12] H. C. Nguyen, R. Amorim, J. Wigard, I. Z. KováCs, T. B. Sørensen, and P. E. Mogensen, "How to ensure reliable connectivity for aerial vehicles over cellular networks," *IEEE Access*, vol. 6, pp. 12 304–12 317, 2018.

[13] T. Izydorczyk, G. Berardinelli, P. Mogensen, M. M. Ginard, J. Wigard, and I. Z. Kovács, "Achieving high UAV uplink throughput by using beamforming on board," *IEEE Access*, vol. 8, pp. 82 528–82 538, 2020.

[14] X. Pang, W. Mei, N. Zhao, and R. Zhang, "Intelligent reflecting surface assisted interference mitigation for cellular-connected UAV," *IEEE Wireless Communications Letters*, vol. 11, no. 8, pp. 1708–1712, 2022.

[15] A. Warrier, S. Al-Rubaye, D. Panagiotakopoulos, G. Inalhan, and A. Tsourdos, "Interference mitigation for 5G-connected UAV using deep Q-learning framework," in *IEEE/AIAA 41st Digital Avionics Systems Conference (DASC)*, 2022, pp. 1–8.

[16] F. K. Hee and M. Mokayef, "Interference mitigation techniques for the operation of unmanned aerial vehicle (UAV)," in *IEEE 5th International Symposium in Robotics and Manufacturing Automation (ROMA)*, 2022, pp. 1–5.

[17] B. Yang, Y. Dang, T. Taleb, S. Shen, and X. Jiang, "Sum rate and max-min rate for cellular-enabled UAV swarm networks," *IEEE Transactions on Vehicular Technology*, pp. 1–11, 2022.

[18] Z. Chen and H. Zhang, "Uplink SINR distribution of terrestrial and aerial users with power control," *IEEE Communications Letters*, vol. 25, no. 8, pp. 2540–2544, 2021.

[19] W. Mei, Q. Wu, and R. Zhang, "Cellular-connected UAV: Uplink association, power control and interference coordination," *IEEE Transactions on Wireless Communications*, vol. 18, no. 11, pp. 5380–5393, 2019.

[20] W. Mei and R. Zhang, "Uplink cooperative interference cancellation for cellular-connected UAV: A quantize-and-forward approach," *IEEE Wireless Communications Letters*, vol. 9, no. 9, pp. 1567–1571, 2020.

[21] L. Liu, S. Zhang, and R. Zhang, "Multi-beam UAV communication in cellular uplink: Cooperative interference cancellation and sum-rate maximization," *IEEE Transactions on Wireless Communications*, vol. 18, no. 10, pp. 4679–4691, 2019.

[22] W. Mei and R. Zhang, "Aerial-ground interference mitigation for cellular-connected UAV," *IEEE Wireless Communications*, vol. 28, no. 1, pp. 167–173, 2021.

[23] M. Mozaffari, X. Lin, and S. Hayes, "Towards 6G with connected sky: UAVs and beyond," arXiv: 2103.01143, 2021.

[24] Federal Aviation Administration, "FAA aerospace forecast: Fiscal years 2020-2040," 2020.

[25] ACJA, GSMA and GUTMA, "LTE aerial profile," Tech. Rep., V1.0.0, Nov. 2020.

[26] M. Mozaffari, W. Saad, M. Bennis, Y. Nam, and M. Debbah, "A tutorial on UAVs for wireless networks: Applications, challenges, and open problems," *IEEE Communications Surveys Tutorials*, vol. 21, no. 3, pp. 2334–2360, 2019.

[27] X. Lin, R. Wiren, S. Euler, A. Sadam, H. Määttänen, S. Muruganathan, S. Gao, Y. . E. Wang, J. Kauppi, Z. Zou, and V. Yajnanarayana, "Mobile network-connected drones: Field trials, simulations, and design insights," *IEEE Vehicular Technology Magazine*, vol. 14, no. 3, pp. 115–125, 2019.

[28] M. M. Azari, G. Geraci, A. Garcia-Rodriguez, and S. Pollin, "UAV-to-UAV communications in cellular networks," *IEEE Transactions on Wireless Communications*, vol. 19, no. 9, pp. 6130–6144, 2020.

[29] M. Mozaffari, X. Lin, and S. Hayes, "Toward 6g with connected sky: UAVs and beyond," *IEEE Communications Magazine*, vol. 59, no. 12, pp. 74–80, 2021.

[30] M. Chiang, C. W. Tan, D. P. Palomar, D. O'neill, and D. Julian, "Power control by geometric programming," *IEEE Transactions on Wireless Communications*, vol. 6, no. 7, pp. 2640–2651, 2007.

[31] L. P. Qian, Y. J. Zhang, and J. Huang, "MAPEL: Achieving global optimality for a non-convex wireless power control problem," *IEEE Transactions on Wireless Communications*, vol. 8, no. 3, pp. 1553–1563, 2009.

[32] C. S. Chen, K. W. Shum, and C. W. Sung, "Round-robin power control for the weighted sum rate maximisation of wireless networks over multiple interfering links," *Eur. Trans. Telecommun.*, vol. 22, pp. 458–470, 2011.

[33] Jianwei Huang, R. A. Berry, and M. L. Honig, "Distributed interference compensation for wireless networks," *IEEE Journal on Selected Areas in Communications*, vol. 24, no. 5, pp. 1074–1084, 2006.

[34] A. Gjendemsjo, D. Gesbert, G. E. Oien, and S. G. Kiani, "Binary power control for sum rate maximization over multiple interfering links," *IEEE Transactions on Wireless Communications*, vol. 7, no. 8, pp. 3164–3173, 2008.

[35] F. Liang, C. Shen, W. Yu, and F. Wu, "Towards optimal power control via ensembling deep neural networks," *IEEE Transactions on Communications*, vol. 68, no. 3, pp. 1760–1776, 2020.

[36] "Enhanced LTE support for aerial vehicles," Tech. Rep., 3GPP TR 36.777 V15.0.0, Jan. 2018.

[37] R. Amorim, H. Nguyen, P. Mogensen, I. Z. Kovács, J. Wigard, and T. B. Sørensen, "Radio channel modeling for UAV communication over cellular networks," *IEEE Wireless Communications Letters*, vol. 6, no. 4, pp. 514–517, 2017.

[38] X. Cai, C. Zhang, J. Rodríguez-Piñeiro, X. Yin, W. Fan, and G. F. Pedersen, "Interference modeling for low-height air-to-ground channels in live LTE networks," *IEEE Antennas and Wireless Propagation Letters*, vol. 18, no. 10, pp. 2011–2015, 2019.

[39] J. Rodríguez-Piñeiro, T. Domínguez-Bolaño, X. Cai, Z. Huang, and X. Yin, "Air-to-ground channel characterization for low-height UAVs in realistic network deployments," *IEEE Transactions on Antennas and Propagation*, vol. 69, no. 2, pp. 992–1006, 2021.

[40] X. Cai, T. Izydorczyk, J. Rodríguez-Piñeiro, I. Z. Kovács, J. Wigard, F. M. L. Tavares, and P. E. Mogensen, "Empirical low-altitude air-to-ground spatial channel characterization for cellular networks connec-tivity," *IEEE Journal on Selected Areas in Communications*, vol. 39, no. 10, pp. 2975–2991, 2021.

[41] W. Khawaja, I. Guvenc, and D. Matolak, "UWB channel sounding and modeling for UAV air-to-ground propagation channels," in *IEEE Global Communications Conference (GLOBECOM)*, 2016, pp. 1–7.

[42] Z. Huang, J. Rodríguez-Piñeiro, T. Domínguez-Bolaño, X. Cai, and X. Yin, "Empirical dynamic modeling for low-altitude UAV propagation channels," *IEEE Transactions on Wireless Communications*, vol. 20, no. 8, pp. 5171–5185, 2021.

[43] X. Cai, X. Yin, X. Cheng, and A. Pérez Yuste, "An empirical random-cluster model for subway channels based on passive measurements in UMTS," *IEEE Transactions on Communications*, vol. 64, no. 8, pp. 3563–3575, 2016.

[44] "Study on channel model for frequencies from 0.5 to 100 GHz," Tech. Rep., 3GPP TR 38.901 V16.1.0, Jan. 2020.

[45] L. Maggi, A. Valcarce, and J. Hoydis, "Bayesian optimization for radio resource management: Open loop power control," *IEEE Journal on Selected Areas in Communications*, vol. 39, no. 7, pp. 1858–1871, 2021.

[46] "NR; User Equipment (UE) radio transmission and reception; Part 1: Range 1 Standalone," Tech. Rep., 3GPP TS 38.101-1 V17.7.0, Oct. 2022.

[47] C. Rosa and K. I. Pedersen, "Performance aspects of LTE uplink with variable load and bursty data traffic," in *21st Annual IEEE International Symposium on Personal, Indoor and Mobile Radio Communications*, 2010, pp. 1871–1875.

[48] S. Lee, I. Pefkianakis, A. Meyerson, S. Xu, and S. Lu, "Proportional fair frequency-domain packet scheduling for 3GPP LTE uplink," in *IEEE INFOCOM 2009*, 2009, pp. 2611–2615.

[49] J. Huang, V. G. Subramanian, R. Agrawal, and R. A. Berry, "Downlink scheduling and resource allocation for OFDM systems," *IEEE Transactions on Wireless Communications*, vol. 8, no. 1, pp. 288–296, 2009.

[50] X. Cai, I. Z. Kovács, J. Wigard, and P. E. Mogensen, "A centralized and scalable uplink power control algorithm in low SINR scenarios," *IEEE Transactions on Vehicular Technology*, vol. 70, no. 9, pp. 9583–9587, 2021.

[51] S. Hosseinalipour, A. Rahmati, D. Y. Eun, and H. Dai, "Energy-aware stochastic UAV-assisted surveillance," *IEEE Transactions on Wireless Communications*, vol. 20, no. 5, pp. 2820–2837, 2021.

[52] R. Mullner, C. F. Ball, K. Ivanov, J. Lienhart, and P. Hric, "Contrasting open-loop and closed-loop power control performance in UTRAN LTE uplink by UE trace analysis," in *IEEE International Conference on Communications*, 2009, pp. 1–6.

[53] "Evolved Universal Terrestrial Radio Access (E-UTRA); Physical layer procedures," Tech. Rep., 3GPP TS 36.213 V17.3.0, Sep. 2022.

[54] D. P. Palomar and M. Chiang, "Alternative distributed algorithms for network utility maximization: Framework and applications," *IEEE Transactions on Automatic Control*, vol. 52, no. 12, pp. 2254–2269, 2007.